OFDM Signals as the Radar Waveform to Solve Doppler Ambiguity

R. FIRAT TIGREK
Aselsan Electronic Industries
Ankara, Turkey

WIM J. A. DE HEIJ
Thales Nederland B.V.
The Netherlands

PIET VAN GENDEREN
Delft University of Technology
The Netherlands

The OFDM communication signal is proposed for spread spectrum radar signal generation. A radar signal processing technique is developed to solve the Doppler ambiguity in the pulsed Doppler radar by exploiting the multicarrier structure of the OFDM and the random phase modulation on the carriers in a Doppler compensation scheme. The novel processing technique is analyzed in detail, through both analytical derivations and Monte Carlo simulations, to demonstrate the feasibility of using the OFDM modulation with random phase coding for radar signals.

Manuscript received October 8, 2009; revised May 3, 2010; released for publication October 8, 2010.

IEEE Log No. T-AES/48/1/943603.

Refereeing of this contribution was handled by R. Narayanan.

This project has received research funding from the Early Stage Training action in the context of the European Community's Sixth Framework Programme.

At the time of release for publication, R. Firat Tigrek was with the International Research Centre for Telecommunications and Radar, Delft University of Technology, Delft, the Netherlands. He is now at Aselsan Electronic Industries in Ankara, Turkey.

Authors' addresses: R. F. Tigrek, Aselsan Electronic Industries, P.K. 1, Yenimahalle, 06172, Ankara, Turkey, E-mail: (rftigrek@gmail.com); W. J. A. de Heij, Thales Netherlands, Haaksbergerstraat 49, 7554 PA, Hengelo, The Netherlands, (Wim.deHeij@nl.thales.com); P. van Genderen, Delft University of Technology, Faculty of EEMCS, Mekelweg 4, 2628CD Delft, The Netherlands, E-mail: (P.vanGenderen@tudelft.nl).

I. INTRODUCTION

The synergy between the radar and the telecommunications areas creates a new potential because of the push for smaller and low-cost telecommunication equipment. The radar systems are also following suit, and new application areas for smaller and low-cost radar units are emerging. A network of radars can exploit the availability of multiple low-cost radar systems to combine the information acquired from multiple radars that view a target from different aspect angles to enhance the target detection and classification. Such a network of radars requires communication links between the radars, which can be very susceptible to interference and disruptions if based on commercially available communication infrastructure.

Integrating the communication capability in the radar system is considered as a robust solution that avoids almost all the vulnerabilities of a commercial communication infrastructure. The integration is not only in the hardware level; the radar signal has double functionality as a communications signal. To this end, we present a radar signal processing method based on the use of the communication signal that is transmitted by the radar itself as the radar signal. The modulation technique that we consider is the orthogonal frequency division multiplexing (OFDM), which offers superior control over the spectrum of the signal because the modulation technique controls the amplitude and the phase of each harmonic component constituting the signal.

When considering the state of the art related to the new radar signal processing result presented in this paper, three distinct features of the proposed method have to be taken into account. The first feature, the use of OFDM signal for radar applications, was first proposed for performance improvement, such as better confined signal spectrum compared with conventional waveforms in [1] and [2] and improved detection performance in [3]. Later, adaptive radar waveform schemes were proposed that were based on the flexibility of the OFDM modulation [4, 5]. However, none of the proposals listed encompasses the communication function that we seek to use for establishing a network of monostatic radars.

The second feature concerns the concept of a network of radars that establish communication links through their directive beams, which has been proposed in [6] and can be considered as seminal for the current paper because it suggests OFDM as the modulation of choice for the communication signal. A continuation of that effort takes into account the directional antenna pattern [7] and a more rigorous modeling of the time-varying channel [8]; all such contributions focused on the OFDM as the communication signal, while the use of OFDM

communication signal as the radar signal was not elaborated upon until now in the context described here.

It must be noted that some passive bistatic radar systems, as defined in [9], have developed processing techniques based on OFDM type of signals, in particular when they exploit such signals broadcasted by radio or communication devices [10]. The widespread current interest in the concept of combining radar and communication function using OFDM modulation must also be noted [11–13].

The third feature, which emerges as an essential improvement over the previous methods, is the power to solve the Doppler ambiguity that is an important characteristic of the pulsed Doppler radars.

The principal method for solving the Doppler ambiguity is to compare the measurements from multiple trains of pulses with different pulse repetition frequency (PRF) or carrier frequency, which results in different Doppler ambiguity. Other novel solutions to the Doppler ambiguity in pulse Doppler radar measurements have been proposed in the literature, where the fundamental concept behind the proposed solutions is the introduction of a diverse source of Doppler information other than the Doppler fast Fourier transform (FFT). However, each proposed method is aimed at a very specific application, such as a network of radars [14] or low-PRF radars aimed at targets with very high velocities [15]. Another method that solves the Doppler ambiguity by using multicarrier pulses does not include coding of the pulses or the coherent integration to improve the Doppler resolution [16].

The novel pulse compression method proposed in this paper is also based on providing a diverse source of Doppler information by measuring the frequency shift in the digital domain during the pulse compression stage, which is accomplished by exploiting the Doppler sensitivity of the OFDM signal. The multicarrier structure of the OFDM communication signal has essentially random starting phases for the carriers, which creates the Doppler sensitivity in the pulse compression that is required to solve the Doppler ambiguity using only one train of pulses with OFDM modulation [17, 18]. Coherent integration of a train of OFDM chips after the pulse compression provides the high resolution Doppler measurement.

The paper progresses by providing in Section II the mathematical definition of the OFDM modulation in a fashion that is easier to use in the radar area. The processing scheme is explained in Section III, relying on matrix operations to demonstrate the processing steps. The random phase coding requires considering the statistical properties of the ambiguity function for the single OFDM chip to assess the performance of the radar signal. The expected value and variance of the ambiguity function are derived and demonstrated through Monte Carlo simulations in Section IV. Section V considers the coherent integration of the train of OFDM chips and gives the explanation of how the proposed technique solves the Doppler ambiguity using the periodic ambiguity function. The accuracy of the OFDM radar signal and the proposed processing technique is demonstrated in Section VI through Monte Carlo simulations. Hence, the progression of the paper is from single chip to a train of OFDM chips, and for each case the signal processing steps and the associated Doppler measurement methods are established, which are followed by the investigation of the statistical properties.

II. DEFINITION OF OFDM SIGNAL

OFDM is a spread-spectrum transmission technique where the signal is made up of multiple carriers. The technique is based on the carriers constituting the signal being mathematically orthogonal as a result of the uniform frequency spacing Δf in between the carriers. Apart from this arrangement in the spectrum of the signal, the orthogonal carrier structure also requires the signal duration to be the inverse of the carrier spacing.

Thus, for clarity, the OFDM signal can be considered as constituted of individual segments of duration $T = 1/\Delta f$; each such segment will henceforth be called an OFDM chip. One OFDM chip can be formulated as the sum of the multiple carriers in complex baseband:

$$p(t) = \sum_{m=0}^{N-1} A_m \exp\{j2\pi m\Delta f t\} \exp\{j\varphi_m\}, \qquad 0 \le t < T \tag{1}$$

where A_m and φ_m are the amplitude and the starting phase, respectively, of the carrier m. These parameters can be determined independently; consequently, the communication messages are transmitted using m-ary phase shift keying (m-PSK) or m-ary quadrature amplitude modulation (m-QAM) modulation techniques on each carrier. For the rest of the paper only m-PSK modulation is considered.

It must be noted that the DC component, while it is omitted in communication applications, is included in (1) to provide a more straightforward structure for the matrices that are defined when describing the pulse compression operation later in the paper.

In communication applications, two consecutive OFDM chips are separated by a guard interval, the duration of which is determined by the length of the communication channel, which is in turn determined by the duration that the multipath reflections in the communication channel take to subside. The guard interval can consist of a period of no transmission; however, the most frequently used guard interval technique may possibly be the cyclic prefix. As the

name implies, the cyclic prefix is the repetition of the end portion of the OFDM chip before the actual chip begins.

The OFDM modulation is implemented by the efficient IFFT, which satisfies the timing relation in (1). The input to the IFFT is the modulation coefficients, that is, $A_m \exp\{j\varphi_m\}$. The guard interval is generated by appending a portion of signal from the end to its beginning, which forms a continuous signal of duration $T(1+\alpha)$, $T\alpha$ being the guard interval duration. Such guard interval is labeled as cyclic prefix. The demodulation is implemented by FFT, where the input is a portion of the signal with duration T. The choice of cyclic prefix as the guard interval translates the delay in the signal into a change in the carrier phases.

III. PROCESSING SCHEME FOR OFDM RADAR SIGNAL

The processing scheme is based on the decoding of the received OFDM waveform by discrete Fourier transform (DFT), which is also the crucial stage of demodulation of the OFDM signals in communications. The modulation symbols on each carrier of the OFDM signal can only be recovered if the signal preserves the orthogonal carrier structure. The carriers are orthogonal only with the proper timing and frequency in the receiver, which is acquired from the received signal using various synchronization techniques [19].

To keep the carriers orthogonal, the receiving of the echoes starts at the same time as the transmission of the actual OFDM chip, that is, after the cyclic prefix ends. This arrangement guarantees that the echoes received from the targets constitute one complete OFDM chip during the DFT time window, with the maximum target range determined by the cyclic prefix duration as

$$T\alpha > \frac{2R_{\max}}{c}. \tag{2}$$

A. Expression for Received Echo

With the constraint of (2) in mind, the received and down-converted echo for a single point target during one DFT window is

$$s(t) = \sum_{m=0}^{N-1} \exp\left\{ \begin{array}{c} j2\pi m\Delta f\left(t\left(1-\frac{2v}{c}\right)-\frac{2R}{c}\right) \\ -j2\pi f_c\frac{2R}{c} - j2\pi f_c t\frac{2v}{c} \end{array} \right\} \exp\{j\varphi_m\} \tag{3}$$

where N is the number of carriers, R is the range, v is the radial velocity of the target defined as the derivative of the range, and f_c is the radio frequency (RF) carrier frequency. The time t is relative to the beginning of the DFT window.

The downconverted signal is to be processed in digital domain; hence, the discrete form of the downconverted signal is obtained by replacing the time variable t with the sampling variable such that

$$t = \frac{nT}{N} = \frac{n}{N\Delta f} \tag{4}$$

where n is the sample number.

For the visibility of the processing steps in the formulations, the signal and the processing steps are expressed in terms of matrix operations on discrete samples as

$$\mathbf{s} = \psi \mathbf{\Gamma} \boldsymbol{\beta} \mathbf{A} \boldsymbol{\varphi} \tag{5}$$

where $\mathbf{s}$ is the column vector representing the time samples of the received echo, and for critical sampling,

$$\psi = \exp\left\{-j2\pi f_c \frac{2R}{c}\right\} \tag{6}$$

$$\mathbf{\Gamma} = \mathrm{diag}\{1, \gamma, \gamma^2, \ldots, \gamma^{N-1}\} \tag{7}$$

$$\gamma = \exp\left\{-j2\pi f_c \frac{2v}{c}\frac{1}{N\Delta f}\right\} \tag{8}$$

$$\boldsymbol{\beta} = \begin{bmatrix} 1 & 1 & 1 & \cdots & 1 \\ 1 & \beta & \beta^2 & & \beta^{N-1} \\ 1 & \beta^2 & \beta^4 & & \beta^{2(N-1)} \\ \vdots & & & \ddots & \vdots \\ 1 & \beta^{N-1} & \beta^{2(N-1)} & \cdots & \beta^{(N-1)^2} \end{bmatrix} \tag{9}$$

$$\beta = \exp\left\{j2\pi\left(1-\frac{2v}{c}\right)\frac{1}{N}\right\} \tag{10}$$

$$\mathbf{A} = \mathrm{diag}\{1, \alpha, \alpha^2, \ldots, \alpha^{N-1}\} \tag{11}$$

$$\alpha = \exp\left\{-j2\pi\Delta f \frac{2R}{c}\right\} \tag{12}$$

$$\boldsymbol{\varphi}^T = [\exp\{j\varphi_0\} \quad \exp\{j\varphi_1\} \cdots \exp\{j\varphi_{N-1}\}]. \tag{13}$$

The $\boldsymbol{\beta}$ matrix is the same as an inverse discrete Fourier transform (IDFT) matrix of the same size when $2v/c \ll 1/N$, which will be the assumption in this paper.

The matrix equations are convenient for clearly showing the structure and order of the different operations that take place in the signal processing. The target parameters that are of interest are in the $\mathbf{\Gamma}$ and $\mathbf{A}$ matrices and also in the ψ term.

B. Pulse Compression Technique

The processing scheme as first described in [17] and [18] starts with the DFT to acquire the spectrum components of the received echo. In communications the spectrum components are the modulation symbols that carry the message; here they contain the velocity and range information as can be seen in (8) and (12), respectively. To recover them, we have to

compensate for the starting phases of the carriers by multiplying them with the complex conjugate of the φ vector.

If the conventional pulse compression scheme were to be followed, the next step would be to obtain the range profile by operating the IDFT on the compensated spectrum. Such operation would give us the correlation of the echo with the transmitted signal. However, the Doppler effect on such a scheme manifests itself as a loss in the pulse compression gain, which is investigated in [20].

The merits of the matrix representation become clear here, for the Doppler effect that causes the gain loss is isolated in the $\mathbf{\Gamma}$ matrix. We add the DFT and the phase compensation operations to the received echo expression in (5) as $\mathbf{F}$ and $\mathbf{P}$ matrices, respectively, to obtain

$$\mathbf{PFs} = \psi \mathbf{PF\Gamma F}^{-1}\mathbf{A}\varphi \tag{14}$$

where $\mathbf{F}^{-1}$ is the IDFT matrix and

$$\mathbf{P} = \text{diag}\{\exp\{-j\varphi_0\},\exp\{-j\varphi_1\},\ldots,\exp\{-j\varphi_{N-1}\}\}. \tag{15}$$

The exponential terms that constitute the $\mathbf{\Gamma}$ matrix are multiplied by the columns of the DFT matrix $\mathbf{F}$. This multiplication corresponds to the cyclic shift of the rows of $\mathbf{F}$ upward by ε when

$$\frac{2v}{c} f_c = \varepsilon \Delta f \tag{16}$$

with ε being an integer. This cyclic shift of the rows of the $\mathbf{F}$ matrix can be compensated for before the phase compensation takes place by multiplication with another matrix $\mathbf{C}_\varepsilon^{-1}$, which is the identity matrix that is cyclically shifted by ε in the opposite direction from $\mathbf{F}$. Thus, the Doppler-compensated range profile is

$$\chi(\varepsilon) = \mathbf{F}^{-1}\mathbf{PC}_\varepsilon^{-1}\mathbf{Fs}. \tag{17}$$

where the column vector $\boldsymbol{\xi}(\varepsilon)$ is the range profile for the cyclic shift ε. For certain pulse compression waveforms, the result of the Doppler effect is a decrease in the pulse compression gain; this is also true for the OFDM communication signals. The Doppler sensitivity arising from the random phase coding of the multicarrier structure and the simple Doppler compensation scheme described earlier are fundamental in solving the Doppler ambiguity. The reason for the Doppler sensitivity and the method of solving the Doppler ambiguity will be explained in the next two sections.

The complete processing scheme is obtained when the particular range cells of the range profiles for the same cyclic shift ε are integrated coherently for the train of pulses via another DFT, which can be expressed as

$$\Lambda(\varepsilon,\theta,\nu) = \sum_{p=0}^{K-1} \chi_p(\varepsilon,\theta)\exp\left\{-j2\pi\frac{p\nu}{K}\right\} \tag{18}$$

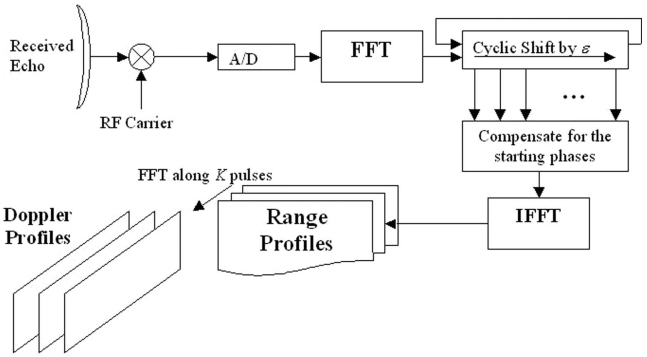

Fig. 1. Complete processing chain that exploits multicarrier structure of OFDM to solve Doppler ambiguity.

where K is the number of pulses that are coherently integrated, $\nu = 0,1,\ldots,K$ is the corresponding Doppler bin of the Doppler DFT output and $\xi_p(\varepsilon,\theta)$ is the entry of the vector $\boldsymbol{\xi}(\varepsilon)$ corresponding to the range bin θ for pulse p. This final operation is the same as that applied in the conventional pulsed Doppler radar to extract the Doppler information. The complete processing scheme is depicted in Fig. 1.

IV. ANALYSIS OF PROCESSING OUTPUT FOR SINGLE OFDM CHIP

The use of communication signals as the radar signal imposes the assumption that the phase codes on the carriers of the OFDM signal are essentially random. As a consequence, the analysis on the pulse compression has to focus on the statistical properties of the ambiguity function, namely the expected value and the variance of the pulse compression output.

An important step is the demonstration of the equivalence of the processing output to the ambiguity function expression that is frequently used to assess the performance of radar signals. This connection, as demonstrated in Appendix A, shows that the investigations on the pulse compression output are comparable with similar investigations of radar signals in the literature.

While the matrix operations are concise, it is hard to evaluate the expected value and the variance of the pulse compression output easily in that form. Thus, the pulse compression is given in a more familiar form as

$$\chi(\varepsilon,\theta) = \frac{1}{N^2}\sum_{k=0}^{N-1}\sum_{n=0}^{N-1}\sum_{m=0}^{N-1}\begin{cases}\exp\left\{j2\pi k\left(\dfrac{\theta}{N}-\dfrac{2R\Delta f}{c}\right)\right\}\\ \exp\left\{-j2\pi f_c\dfrac{2v}{c}\dfrac{n}{N\Delta f}\right\}\\ \exp\left\{j2\pi\dfrac{(m-k-\varepsilon)n}{N}\right\}\\ \exp\{j(\varphi_m-\varphi_k)\}\end{cases}. \tag{19}$$

A. Expected Value and Variance of Pulse Compression

The expected value is more easily evaluated in the form in (19), thanks to the random phase terms being explicit in the equation. The expected value for the pulse compression output can then be written as

$$E[\chi(\varepsilon,\theta)] = \frac{1}{N^2}\sum_{k=0}^{N-1}\sum_{n=0}^{N-1}\sum_{m=0}^{N-1}\begin{cases}\exp\left\{j2\pi k\left(\dfrac{\theta}{N}-\dfrac{2R\Delta f}{c}\right)\right\}\\ \exp\left\{-j2\pi f_c\dfrac{2v}{c}\dfrac{n}{N\Delta f}\right\}\\ \exp\left\{j2\pi\dfrac{(m-k-\varepsilon)n}{N}\right\}\\ E[\exp\{j(\varphi_m-\varphi_k)\}]\end{cases}. \tag{20}$$

The assumption that the phases are random with uniform distribution leads to the expected value

$$E[\exp\{j(\varphi_m-\varphi_k)\}] = \begin{cases}0, & m\neq k\\ 1, & m=k\end{cases} \tag{21}$$

which leads to

$$E[\chi(\varepsilon,\theta)] = \frac{1}{N^2}\sum_{k=0}^{N-1}\sum_{n=0}^{N-1}\begin{cases}\exp\left\{j2\pi k\left(\dfrac{\theta}{N}-\dfrac{2R\Delta f}{c}\right)\right\}\\ \exp\left\{-j2\pi f_c\dfrac{2v}{c}\dfrac{n}{N\Delta f}\right\}\\ \exp\left\{-j2\pi\dfrac{\varepsilon n}{N}\right\}\end{cases}. \tag{22}$$

The variance of the side lobes is defined as

$$\sigma_\chi^2 = E[|\chi|^2]-|E[\chi]|^2. \tag{23}$$

For brevity the derivation of the variance is given in the Appendix B. The final expression for the variance is

$$\sigma^2_{\chi(\varepsilon,\theta)} = \frac{1}{N^4}\sum_{k=0}^{N-1}\sum_{n=0}^{N-1}\sum_{m=0m\neq k}^{N-1}\sum_{\bar{n}=0}^{N-1}\begin{cases}\exp\left\{j2\pi\dfrac{(m-k-\varepsilon)(n-\bar{n})}{N}\right\}\\ \exp\left\{-j2\pi f_c\dfrac{2v}{c}\dfrac{(n-\bar{n})}{N\Delta f}\right\}\end{cases}. \tag{24}$$

The random behavior of the pulse compression becomes evident once a number of OFDM chips with random starting phases of the carriers are generated and processed. Monte Carlo simulations are carried out in MATLAB to validate the analytical derivations, where the OFDM signal echo with $N = 128$ carriers is generated according to (5). The matrix formulation of (5) is implemented by replacing the $\boldsymbol{\beta}$ matrix with the IDFT matrix, which is in turn implemented by the IFFT algorithm. The target range and velocity are taken to be zero, with no loss of validity due to the equivalence of the OFDM pulse compression and the ambiguity function. The starting phases of OFDM carriers are randomly generated with uniform distribution over the available phase states that constitute the quadrature phase shift keying (QPSK) phase constellation.

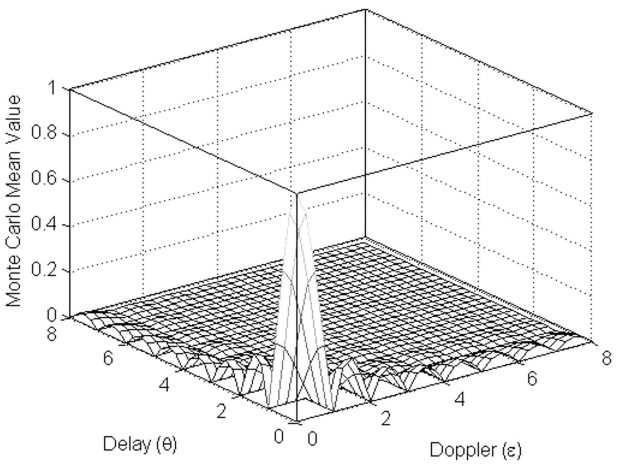

Fig. 2. Mean value of pulse compression output for single OFDM chip of 128 carriers, generated through Monte Carlo simulations.

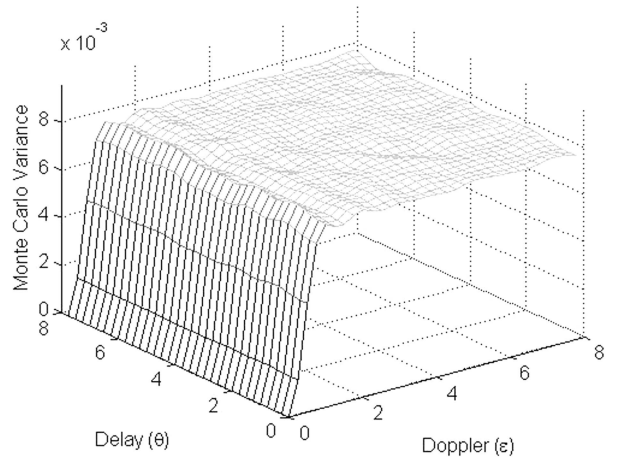

Fig. 3. Variance of pulse compression output for single OFDM chip of 128 carriers, generated through Monte Carlo simulations.

The mean value calculated from the Monte Carlo simulations is depicted in Fig. 2. The $\sin(x)/x$ shapes along the delay and Doppler frequency axes are clearly visible, which matches the absolute value of the expected value expression in (22). The same $\sin(x)/x$ shape along the delay and the Doppler axes is also derived in [20].

The variance is also calculated from the Monte Carlo simulations and plotted in Fig. 3, which resembles the behavior of the pulse compression for noise waveforms. An investigation of the statistical properties for the autocorrelation of the noise waveforms in [21] shows that the random time domain samples give rise to random side lobes of the autocorrelation function. The noiselike effect of the random components in the transmitted signal is described as correlation noise.

One characteristic feature of the novel pulse compression scheme that is clearly visible in Fig. 3

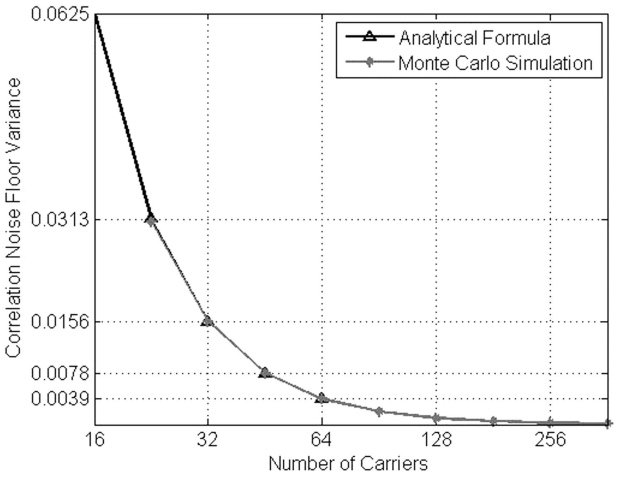

Fig. 4. Variance of the normalized correlation noise floor for pulse compression of single OFDM chip versus number of carriers.

is the zero variance along the zero-Doppler range cut, which corresponds to the autocorrelation of the waveform. This feature is due to the flat power spectrum of the OFDM when the carriers are m-PSK modulated. The lack of correlation noise in the autocorrelation function may also provide an advantage in the detection of slowly moving ground targets by reducing the interference from stationary ground clutter. This property is also observed when the variance expression in (24) is plotted numerically.

Both the Monte Carlo simulations and the analytical expression in (24) show that the variance of the side lobes converges to a certain value with the Doppler shift further away from the compensated value. This convergence value for the variance is plotted with respect to the number of carriers, as calculated from the analytical formula in (24) and from the Monte Carlo simulations in Fig. 4. There is an excellent matching of the values derived from both methods, and the relation between the value to which the variance converges and the number of carriers N is revealed to be

$$\sigma^2_{\chi,N} = \frac{1}{N}. \tag{25}$$

Note that this variance level is considered for the ambiguity function with unity peak.

B. Contribution of Additive White Gaussian Noise to Variance of Processing Output

Besides the random starting phases of the carriers, the additive white Gaussian (AWG) noise also has an effect on the pulse compression, which can be included in the derivations of the expected value and the variance easily through two assumptions:

1) *Assumption 1*: The expected value for the noise alone is zero. This assumption is useful because the pulse compression operation is linear; the output of the pulse compression for the AWG noise is eliminated when considering the expected value of the pulse compression.

2) *Assumption 2*: The AWG noise and the signal are independent and uncorrelated. When considering the variance of the pulse compression output, the correlation of the noise and received echo appears in the expected value of the squared processing output. This assumption eliminates the cross-correlation terms, leaving the final expression for the variance as

$$\sigma^2 = \sigma^2_{\chi(\varepsilon,\theta)} + \sigma^2_{\mathrm{AWG}}. \tag{26}$$

This equation can be modified to include the signal-to-noise ratio (SNR). If the signal power is considered as 0 dBW, the noise variance, which is the expected value for the noise power, is equal to 1/SNR.

The variance for the correlation noise is calculated for signal energy normalized to 1 to yield a unity ambiguity function peak. The OFDM pulse compression presented in this paper and the ambiguity function are equivalent, as demonstrated in Appendix A. Therefore, the variance calculated from (19) is valid for the normalized ambiguity function.

The ratio of signal energy to the average signal power is N for critically sampled OFDM; thus, the noise variance for the energy-normalized signal for the same SNR is

$$\sigma^2_{\mathrm{AWG}} = \frac{1}{N \times \mathrm{SNR}}. \tag{27}$$

After also substituting (25) and (27) in (26), the variance of the ambiguity function for critically sampled baseband OFDM converges to

$$\sigma^2 = \frac{1 + 1/\mathrm{SNR}}{N} \tag{28a}$$

where SNR is the signal-to-noise ratio in linear scale. However, this SNR is for the received signal before the pulse compression; the correlation noise is calculated for the output of the pulse compression, and for a meaningful comparison the SNR after the pulse compression has to be considered. The pulse compression gain is determined by the time-bandwidth product, which is equal to the number of carriers N for the OFDM signal. Hence, the variance term in (28) can be reorganized to include the SNR after the pulse compression as

$$\sigma^2 = \frac{1}{N} + \frac{1}{\mathrm{SNR}_{PC}} \tag{28b}$$

where $\mathrm{SNR}_{PC} = N \cdot \mathrm{SNR}$. As the SNR increases, the correlation noise becomes dominant, and with decreasing SNR, the noise variance is the greatest contributor to the variance of the ambiguity function side lobes.

As pointed out in (26), the thermal noise and the correlation noise variances add up because the two noise contributions are uncorrelated. The main difference between the AWG noise floor and

the correlation noise floor is that the latter is also determined by the strongest echo received from the reflecting agents when there are multiple reflecting objects.

V. COHERENT INTEGRATION OF TRAIN OF OFDM CHIPS AND SOLVING DOPPLER AMBIGUITY

The structure of the multicarrier signal and the unique outcome of the novel processing technique offer a new solution to the ambiguity in the Doppler measurements. As explained in the previous section, the Doppler effect in the pulse compression can be observed as the shift of the spectrum components of the received echo relative to that of the transmitted OFDM signal.

The importance of this feature of the waveform comes from the required time on target to achieve certain Doppler resolution without any ambiguity. The duration of the burst of pulses that are integrated coherently determines the Doppler resolution. However, the PRF introduces ambiguity to both the delay and the Doppler axes of the ambiguity function, and alleviating the ambiguity along one axis aggravates the ambiguity along the other axis.

When multiple bursts of pulses with different PRF are transmitted to solve the ambiguity in Doppler, the time the radar beam has to dwell on the target is also multiplied. For radar systems using rotating antennas, the radar beam width has to be kept broad; hence, the azimuth resolution of the radar is sacrificed to solve the Doppler ambiguity. The OFDM radar signal and the proposed processing technique solve this dilemma by exploiting the Doppler sensitivity in the pulse compression.

The use of random phases with uniform distribution creates sensitivity in the pulse compression gain against the Doppler shift [17]. The processing can be regarded as combining the result of the pulsed Doppler processing with the Doppler sensitive response of the pulse compression. The whole process can be understood better when the periodic ambiguity function (PAF) for the pulse burst is considered.

The PAF, as described in [22], is devised as a means of investigating the waveforms consisting of coherent identical pulses. Obviously the pulse burst consisting of OFDM chips with random phases does not fulfill the conditions under which the use of PAF is valid. However, the guard interval being implemented as cyclic prefix allows the use of PAF with the condition that the delay under consideration is less than the guard interval duration. Hence, the PAF expression as given in [22] can be used justifiably,

$$|\chi(\tau, f_d)| = |\chi_T(\tau, f_d)| \left| \frac{\sin(K\pi f_d T(1+\alpha))}{K \sin(\pi f_d T(1+\alpha))} \right| \quad (29)$$

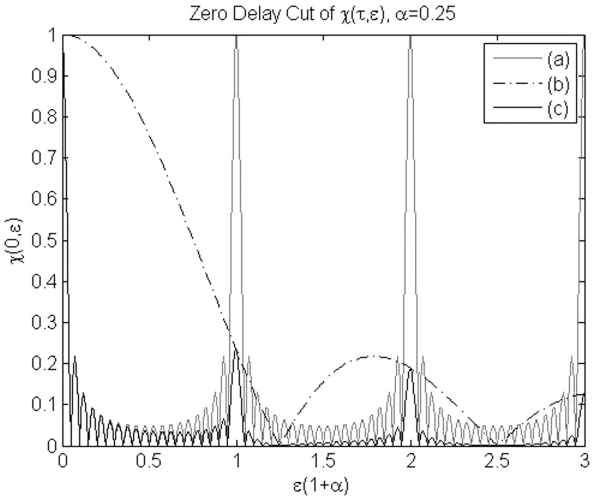

Fig. 5. Expected zero delay Doppler cut of ambiguity functions of (a) the unmodulated pulse train, (b) single OFDM pulse modulated with uniformly distributed random phases, (c) train of such OFDM pulses.

where $|\xi_T(\tau, f_d)|$ is the single-period PAF, the ambiguity function for the single OFDM chip, which is shown in Appendix A to be equivalent to the processing output. The random nature of the OFDM chips imposes the use of the expected value of the pulse compression response, as given in (22).

Fig. 5 shows the absolute value of the expression given in (22) with zero delay placed over the zero delay cut of the PAF for the unmodulated pulse train. The Doppler sensitivity arising from the use of the random phases with uniform distribution is clearly visible in the pulse compression result for the single OFDM chip. The way this sensitivity is used to solve the Doppler ambiguity is demonstrated in the PAF for the OFDM pulse train. The ambiguous response from the pulsed Doppler processing, which is labeled (b) in Fig. 5, is masked by the Doppler sensitive pulse compression response for the single OFDM chip, which is labeled (a) in Fig. 5, to yield the final response for the signal processing, which is labeled (c) in Fig. 5.

The $\sin(x)/x$ shape in Fig. 5, which can be recognized as the Doppler cut of the expected value in Fig. 2, is the result of the displacement of the OFDM carriers due to Doppler shift. Autocorrelation of the sequence of uniformly distributed random phases yields a single high peak while side lobes are much lower. Thus, the autocorrelation peak occurs when the cyclic shift of the OFDM carriers by ε during the pulse compression matches the displacement of the carriers due to the Doppler shift.

The Doppler ambiguity is solved by comparing the amplitudes of different cyclic shifts for the range and Doppler FFT bin in which the target is detected; the cyclic shift value ε that yields the highest amplitude corresponds to an unambiguous, low-resolution Doppler measurement, which can be combined with

the folded-over high resolution Doppler measurement to solve the Doppler ambiguity.

VI. MEASUREMENT ACCURACY

As explained in the previous section, modulating the carriers using uniformly distributed random phase codes is essential for alleviating the ambiguity in the Doppler measurements. The randomness of the modulation components compels us to consider the statistical properties of the processing output; hence, the expected value of the ambiguity function is used when demonstrating the approach for alleviating the Doppler ambiguity in the previous section.

The random nature of the OFDM waveform can be considered as akin to that of the noise radar waveforms. One investigation of the noise radar waveforms [21] shows the effects of the randomness of the waveform on the autocorrelation function; the random fluctuations in the autocorrelation establish a noise floor, which limits the sensitivity of the radar. Moreover, the random fluctuations will also have an effect essentially similar to that of the thermal noise on the accuracy of the measurements.

Assessing the accuracy with which the radar measures the target parameters requires the adoption of an estimation technique. The discrete range and Doppler bins usually do not coincide with the actual target parameters, resulting in the straddling loss in the pulse compression gain and preventing the accurate measurement of the target parameters. Oversampling and various estimation and interpolation techniques are adopted to prevent the straddling loss. However, assessing different interpolation and estimation techniques for the novel pulse compression technique is out of the scope of this paper.

Instead of developing an interpolation technique that is based on linear regression or least squared error curve fitting techniques, we adopt the sinc interpolation and numerically determine the peak location for simulated targets. The sinc interpolation reconstructs a signal from its samples by summing the sample-weighted sinc functions such as

$$f(t) = \sum_{n=-\infty}^{\infty} x_n \mathrm{sinc}(\pi(t - nT)) \tag{30}$$

where x_n are the discrete samples, T is the sampling period, and f(t) is the interpolated signal. The delay and Doppler values, where the peak of the interpolated processing output is located, corresponds to the actual target parameters.

Instead of continuous time variable t, discrete time variable with sampling period much shorter than T is submitted such that the sampling rate is increased significantly to reduce the error arising from the straddling. The sample with the greatest amplitude and the two adjacent samples on each side are taken into account for the interpolation because the curve fitting techniques described in the literature are also based on a few samples around the maximum [23, 24].

The interpolation is considered separately for the delay and the Doppler FFT outputs for the cyclic shift that corresponds to the target velocity to determine the accuracy of the target parameter measurement. Thus, the interpolation is conducted in one dimension (1-D) at a time; the techniques using 2-D functions for interpolation can be considered as well. The accuracy in solving the Doppler ambiguity is assessed separately by focusing on the range bin at which the target is present and comparing the Doppler FFT outputs and the cyclic shift results.

TABLE I
Common Waveform and Target Parameters for the Simulations

Parameter Name	Parameter Value	Parameter Name	Parameter Value
Carrier spacing	1 kHz	Coherent integration time	21.6 ms
Number of carriers	10^3	Range resolution	150 m
RF carrier frequency	10 GHz	Velocity resolution	0.69444 m/s

TABLE II
Waveform and Target Parameters for Evaluating the Guard Interval Effect

Parameter Name	Simulation I	Simulation II	Simulation III
Number of pulses	15	18	20
Guard interval relative duration	0.44	0.20	0.08
Target range interval (m)	$375 \le R \le 525$	$375 \le R \le 525$	$375 \le R \le 525$
Target velocity interval (m/s)	$0 \le v \le 375$	$0 \le v \le 375$	$0 \le v \le 375$

A. Parameter Selection for Monte Carlo Simulations

To verify the relation between the Doppler ambiguity and the guard interval duration, we determined three different waveform parameters for which Monte Carlo simulations are performed. The primary constraint when determining the waveform parameters was keeping the range and Doppler resolution the same for each parameter set while obtaining an integer number of samples for the guard interval and the number of pulses. Such constraints yielded a very limited parameter set, which are given in Tables I and II. It must be noted that the guard interval duration $\alpha = 0.44$ is far from realistic; however, it is included in the Monte Carlo simulations to clearly demonstrate the relation between α and the rate of ambiguity solving success.

Other parameters that are crucial in obtaining meaningful Monte Carlo results are the range and velocity of the simulated point target, which are randomly determined for each run. For the range, the outcome of the signal processing is repetitive for each

range cell. Thus, range is randomly determined such that it is uniformly distributed between the last half of one range cell and the next half of the following, covering all the range bin straddling cases possible for one range bin.

Determining the velocity is more complicated because there are two separate processing steps that have repetitive results with different periods. The result of the Doppler FFT is repetitive for velocity after the Doppler ambiguity is reached, while the result for the cyclic shift is repetitive for each cyclic shift bin. The least common multiple (LCM) of the repetition periods is determined for each parameter set in Table II, and the velocity is randomly chosen to obtain a uniform distribution between zero and the LCM velocity. Note that while the LCM velocity for $\alpha = 0.2$ is 75 m/s, to keep the size of the velocity intervals the same for all pulses, we have chosen 375 m/s as the upper limit.

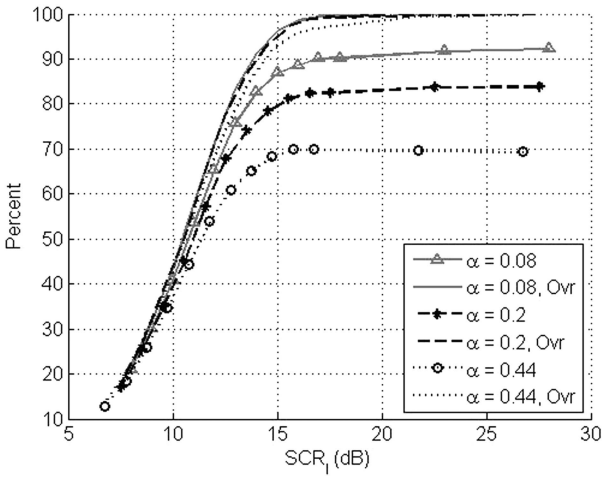

Fig. 6. Number of unambiguous velocity measurement as percentage versus SNR after coherent Doppler integration in decibels for three different guard interval durations, without and with oversampling by factor of 2.

B. Monte Carlo Simulation Results

To see the effect of correlation noise and additive white Gaussian noise (AWGN) on the accuracy of the processing and interpolation techniques, we performed Monte Carlo simulations for different SNR levels. Two sets of results are generated to demonstrate the accuracy of both the Doppler ambiguity solutions and the range and ambiguous velocity measurements.

The number of ambiguous velocity estimations for various SNR_I (the SNR after coherent Doppler integration) and guard interval durations is plotted in Fig. 6. The Doppler ambiguity is solved by forming a list of ambiguous velocities that correspond to the Doppler FFT bin in which the target is present and choosing among this list the velocity that is the closest to the velocity that corresponds to the cyclic shift that yields the highest pulse compression gain. Both the FFT bin and the cyclic shift corresponding to the target velocity are determined by a peak search in the pulse compression response. More advanced estimation methods, while they may possibly yield better results, are outside the scope of this paper. The greatly increased percentage of ambiguous velocity estimations for longer guard interval durations verifies the assessment of [18] that the Doppler ambiguity is solved better when the relative duration of the guard interval is smaller. Fig. 6 also shows that oversampling the cyclic shift results by a factor of 2 corrects the ambiguous estimations, which is thanks to more accurate determination of the peak position for the pulse compression gain with respect to the amount of cyclic shift. It is observed that further increase in the oversampling does not give further improvement.

An important feature observed in Fig. 6 is the relatively rapid decrease in the percentage of correct solutions when SNR_I is reduced below 15 dB. The reduction is dominated by erroneous measurements of the velocity rather than the Doppler ambiguity. Such behavior is expected because of the use of the peak search for finding the target velocity. Below a certain SNR value, a spurious peak due to the noise comes up with amplitude higher than the target response, and coupled with the size of the data set that is the output of the signal processing, the peak search method yields erroneous measurement as the SNR decreases below a threshold determined by the size of the data set.

Accuracies of the range and ambiguous velocity measurements are assessed by focusing on the cyclic shift that yields the highest pulse compression gain; in other words, the one that corresponds to the actual target velocity. The error distributions for the range and velocity measurements are depicted in Figs. 7 and 8, respectively, which feature the combination of estimation errors coming from the interpolation technique and the correlation noise and AWGN.

The distribution of errors for the low-noise case resembles a uniform distribution, while the features of the error distribution increasingly resemble that of the normal distribution as the SNR decreases. A numerical experiment evaluating the distribution of the sum of two random variables, one with uniform distribution and other with normal distribution, yields similar features. Thus, this peculiar feature of the error distribution is due to the separate errors arising from the interpolation technique and the AWGN.

VII. CONCLUSION

We developed a novel processing technique that exploits the Doppler sensitivity arising from the multicarrier structure of the OFDM, where starting phases of the carriers are random with uniform distribution, to solve the Doppler ambiguity. The use of a random phase modulated communication signal

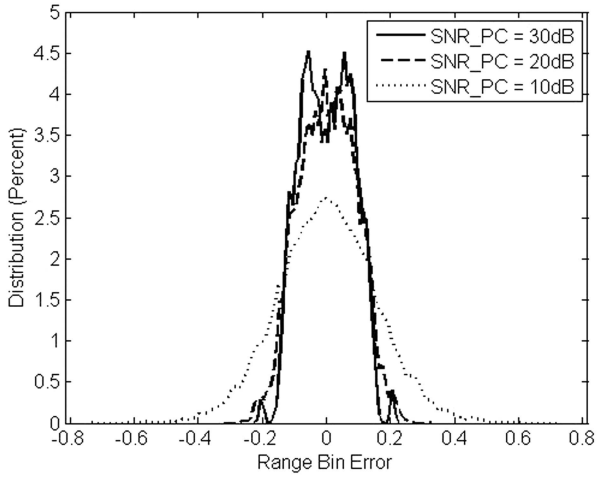

Fig. 7. Distribution of range bin estimation errors for different SNR, for $\alpha = 0.2$.

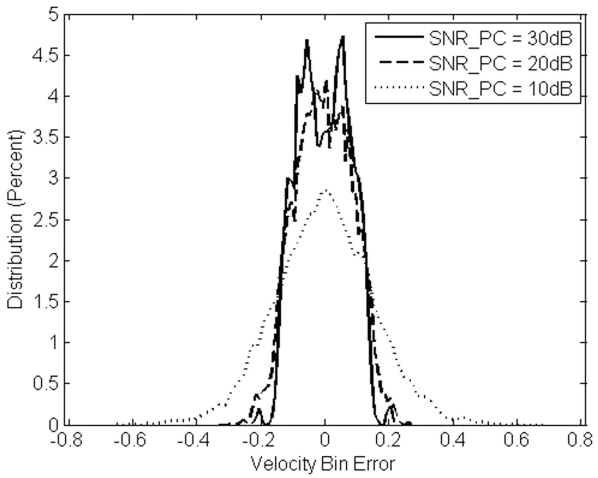

Fig. 8. Distribution of velocity bin estimation errors for different SNR, for $\alpha = 0.2$.

enables conveying communication messages using the radar signal itself; different from the other techniques proposed in the literature, there is no resource sharing and therefore no associated degradation of the radar performance. The monostatic operation translates into perfect knowledge of the transmitted signal, a feature that passive radar systems lack.

The Doppler ambiguity is solved by exploiting the Doppler sensitivity of the random-phase modulated OFDM signal. The Doppler frequency shift manifests itself as a shift of the carrier locations in the spectrum, which is compensated for by the cyclic shift of the spectrum components before the pulse compression. The signal processing technique is simplified further because the pulse compression is accomplished in frequency domain thanks to the cyclic nature of the OFDM signal.

The tool for evaluating the performance of the radar signal and the processing technique is the ambiguity function; however, the random coding requires focusing on the statistical properties of the ambiguity function. Analytical formulations for the expected value and the variance of the ambiguity function are validated through Monte Carlo simulations. Different from the noise radars that modulate the time domain signal with noise, the autocorrelation function (which is the zero-Doppler cut of the ambiguity function) of the random phase modulated OFDM does not exhibit the correlation noise floor, which translates into reduced interference from stationary clutter when searching for slow moving targets.

The results are validated through Monte Carlo simulations that involve random target range and velocity as well as random phase coding. The parameters that have to be engineered to the scenarios of interest are the carrier spacing and the associated OFDM chip duration, the duration of the guard interval relative to the OFDM chip duration, and the number of carriers. The OFDM chip duration and the number of carriers affect the velocity and range resolution, while the effects of modifying the guard interval are demonstrated through both analytical formulations and Monte Carlo simulations.

The complexity associated with the use of the OFDM waveform in radar applications arises from its nonunity peak to average power ratio (PAPR), which prohibits the use of efficient class C amplifiers and imposes power back off to keep the amplifiers operating in their linear regime. To limit the back off and improve the efficiency of the amplifiers, we have to limit the PAPR. There is rich literature regarding this aspect of the OFDM waveform; an overview of the PAPR-limiting techniques can be found in [25]. Future research on the OFDM radar signals has to consider effects of high PAPR as well.

The OFDM communication signal is, hence, shown to be a viable choice for radar signal that incorporates communication capacity, with the additional capability to solve the Doppler ambiguity through the novel signal processing technique. Monte Carlo simulations focusing on the measurement of the target range and velocity also demonstrate the accuracy of the signal processing technique. The increasing signal processing power makes the presented signal processing technique feasible for much larger bandwidths to obtain a high range resolution, along with the high Doppler resolution provided by the coherent integration of a train of OFDM chips.

APPENDIX A. EQUIVALENCE OF PULSE COMPRESSION OUTPUT TO AMBIGUITY FUNCTION

A. Justification of Use of Narrowband Ambiguity Function

The Doppler effect in reality is the scaling of the radar signal echo, in both time domain and frequency

domain, due to the radial velocity of the target. The actual scaling factor is simplified into the form used in (3) by virtue of the assumption $v \ll c$. However, the narrowband ambiguity function can be utilized for evaluating the performance of a radar signal only if the Doppler effect can be modeled accurately as frequency shift rather than scaling, in other words, when the scaling is very small compared with the critical sampling period according to the Nyquist criterion in the digital processing. This condition is formulated as

$$T\frac{2v}{c} \ll \frac{T}{N} \tag{31}$$

where the sampling period on the right-hand side is taken from (4) and the velocity term is taken from the scaling coefficient in (3). Another approach is presented in [21], where the criterion is to limit the range migration during the correlation time by the range resolution of the radar signal; the same condition as (31) is derived for using the Woodward ambiguity function. Hence, the narrowband condition concerns not just the instantaneous bandwidth of the radar signal; the time-bandwidth product has to be considered in relation to the maximum radial velocity of interest.

B. Demonstration of Equivalence

To demonstrate the equivalence of the ambiguity function and the pulse compression output given in (17), we adopt the assumption of zero target velocity and range, which is inherent in the ambiguity function expression. The resulting pulse compression expression contains the received echo

$$\mathbf{s}_0 = \mathbf{F}^{-1}\boldsymbol{\varphi} = \mathbf{p}_t \tag{32}$$

where the other components $\mathbf{A}$, $\boldsymbol{\Gamma}$, and ψ are eliminated through the zero range and velocity assumption, and the resulting signal is nothing but the transmitted time domain signal described in (1), which is written in vector form as $\mathbf{p}_t$.

The next step is to rearrange the OFDM pulse compression expression into

$$\boldsymbol{\chi}(\varepsilon) = \mathbf{F}^{-1}[\boldsymbol{\varphi}^* \otimes (\mathbf{C}_\varepsilon^{-1}\mathbf{F}\mathbf{p}_t)] \tag{33}$$

where $\boldsymbol{\varphi}^*$ is the complex conjugate of the column phase vector defined in (13). The rearrangement in (33) exploits the fact that the $\mathbf{P}$ matrix is diagonal, and the matrix multiplication with such the diagonal matrix on the left can be rearranged into a Hadamard multiplication with a column vector as seen in (33).

At this stage the structure gives more insight into the essence of the pulse compression operation, that it is indeed the matched filtering implemented in frequency domain. We make use of the fact that the cyclic convolution is equal to the inverse discrete Fourier transform of the pointwise multiplication of spectrum components [26].

To realize the connection stated above, we have to eliminate the presence of the cyclic shift matrix $\mathbf{C}_\varepsilon^{-1}$. This is achieved by translating the cyclic shift of the $\mathbf{F}$ matrix into a multiplication from the right-hand side by a diagonal $\boldsymbol{\Gamma}_\varepsilon$ matrix, which is defined in the same manner as in (7), but with coefficients

$$\gamma_\varepsilon = \exp\left\{-j2\pi\frac{\varepsilon}{N}\right\}. \tag{34}$$

The reasoning behind this translation is explained when deriving (17).

Another translation concerns the $\boldsymbol{\varphi}^*$ vector, which has to be rewritten as the discrete Fourier transform of the transmitted signal described in (1). With these two translations, the OFDM pulse compression expression becomes

$$\boldsymbol{\chi}(\varepsilon) = \mathbf{F}^{-1}[(\mathbf{F}\mathbf{p}_t^*) \otimes (\mathbf{F}\boldsymbol{\Gamma}_\varepsilon\mathbf{p}_t)]. \tag{35}$$

In time domain, the OFDM pulse compression is

$$\boldsymbol{\chi}(\varepsilon) = (\mathbf{p}_t^*)_c\boldsymbol{\Gamma}_\varepsilon\mathbf{p}_t \tag{36}$$

where the $(.)_c$ corresponds to a circulant matrix consisting of columns that are cyclically shifted versions of the vector inside the parentheses [26]. For the correlation operation in matched filtering the cyclic shifting moves the elements of the vector upwards.

The final step involves considering one element of the OFDM pulse compression vector

$$\boldsymbol{\chi}(\varepsilon,\theta) = \sum_{\tau=0}^{N-1} p(\theta)^* p(\theta+\tau)\exp\left\{-j2\pi\frac{\varepsilon}{N}\tau\right\} \tag{37}$$

where τ is the index for the columns of the circulant matrix. The expression in (37) corresponds to a particular delay gate θ and a particular Doppler bin ε, which is the discrete form of the ambiguity function expression in [27]. The exponential term is supplied by the $\boldsymbol{\Gamma}_\varepsilon$ matrix, while the τ is introduced by the cyclical shifting in the circulant matrix. Because the OFDM signal is cyclically repeating itself, as evident from the implementation of the cyclic prefix guard interval, we can add that $p(\theta+\tau)$ folds over for $\theta+\tau \gg N-1$.

Note that the ambiguity function as defined in [9] is different from the one defined in [27]. The difference is in the sign of the exponential component and is of no consequence because the squared magnitude of the function in (36) is considered for assessing radar signal performance, which is symmetric with respect to the zero delay and Doppler.

APPENDIX B. THE VARIANCE OF THE PULSE COMPRESSION OUTPUT

The second moment of the pulse compression output is given as

$$E[|\chi(\varepsilon,\theta)|^2] = \frac{1}{N^4}\sum_{k=0}^{N-1}\sum_{n=0}^{N-1}\sum_{m=0}^{N-1}\sum_{\bar{k}=0}^{N-1}\sum_{\bar{n}=0}^{N-1}\sum_{\bar{m}=0}^{N-1}\begin{cases}\exp\left\{j2\pi(k-\bar{k})\left(\frac{\theta}{N}-\frac{2R\Delta f}{c}\right)\right\}\exp\left\{j2\pi\frac{(m-k-\varepsilon)n-(\bar{m}-\bar{k}-\varepsilon)\bar{n}}{N}\right\}\\ \exp\left\{-j2\pi f_c\frac{2v}{c}\frac{(n-\bar{n})}{N\Delta f}\right\}E\{\exp\{j(\varphi_m-\varphi_k-\varphi_{\bar{m}}+\varphi_{\bar{k}})\}\}\end{cases}. \tag{38}$$

The expected value for the phase expression in (38) can be simplified in a similar fashion to (21) as

$$E[\exp\{j(\varphi_m-\varphi_k-\varphi_{\bar{m}}+\varphi_{\bar{k}})\}] = \begin{cases}1, & m=k,\quad \bar{m}=\bar{k}\\ 1, & m=\bar{m},\quad k=\bar{k}\\ 0, & \text{otherwise}\end{cases} \tag{39}$$

which help simplify (38) into

$$\begin{aligned}E[|\chi(\varepsilon,\theta)|^2] = {}& \frac{1}{N^4}\sum_{k=0}^{N-1}\sum_{n=0}^{N-1}\sum_{m=0m\neq k}^{N-1}\sum_{\bar{n}=0}^{N-1}\begin{cases}\exp\left\{j2\pi\frac{(m-k-\varepsilon)(n-\bar{n})}{N}\right\}\\ \exp\left\{-j2\pi f_c\frac{2v}{c}\frac{(n-\bar{n})}{N\Delta f}\right\}\end{cases}\\ &+\frac{1}{N^4}\sum_{k=0}^{N-1}\sum_{n=0}^{N-1}\sum_{\bar{k}=0}^{N-1}\sum_{\bar{n}=0}^{N-1}\begin{cases}\exp\left\{j2\pi(k-\bar{k})\left(\frac{\theta}{N}-\frac{2R\Delta f}{c}\right)\right\}\\ \exp\left\{j2\pi\frac{\varepsilon(\bar{n}-n)}{N}\right\}\\ \exp\left\{-j2\pi f_c\frac{2v}{c}\frac{(n-\bar{n})}{N\Delta f}\right\}\end{cases}.\end{aligned} \tag{40}$$

The second set of summations in (40) is the same as the square of the expected value in (22). Thus, combining (40) and the square of (22) in (23) yields the variance as

$$\sigma^2_{\chi(\varepsilon,\theta)} = \frac{1}{N^4}\sum_{k=0}^{N-1}\sum_{n=0}^{N-1}\sum_{m=0m\neq k}^{N-1}\sum_{\bar{n}=0}^{N-1}\begin{cases}\exp\left\{j2\pi\frac{(m-k-\varepsilon)(n-\bar{n})}{N}\right\}\\ \exp\left\{-j2\pi f_c\frac{2v}{c}\frac{(n-\bar{n})}{N\Delta f}\right\}\end{cases}. \tag{41}$$

ACKNOWLEDGMENTS

This project has received research funding from the Early Stage Training action in the context of the European Community's Sixth Framework Programme. The paper reflects the authors' views, and the European Community is not liable for any use that may be made of the information contained herein.

REFERENCES

[1] Levanon, N.
Multifrequency Signal Structure for Radar Systems.
U.S. Patent 6 392 588, May 21, 2002.

[2] Levanon, N. and Mozeson, E.
Multicarrier radar signal—pulse train and CW.
IEEE Transactions on Aerospace and Electronic Systems, **38**, 2 (Apr. 2002), 707–720.

[3] Prasad, N., Shameem, V., Desai, U. B., and Merchant, S. N.
Improvement in target detection performance of pulse coded Doppler radar based on multicarrier modulation with fast Fourier transform (FFT).
IEE Proceedings on Radar Sonar Navigation, **151**, 1 (Feb. 2004), 11–17.

[4] Sebt, M. A., Norouzi, Y., Sheikhi, A., and Nayebi, M. M.
OFDM radar signal design with optimized ambiguity function.
In *Proceedings of IEEE Radar Conference, RADAR'08*, Rome, Italy, May 26–30, 2008, 448–452.

[5] Sen, S., Hurtado, M., and Nehorai, A.
Adaptive OFDM radar for detecting a moving target in urban scenarios.
In *Proceedings of 2009 International Waveform Diversity and Design Conference*, Orlando, FL, Feb. 8–13, 2009, 268–272.

[6] van Genderen, P. and Nikookar, H.
Radar network communication.
In *Proceedings of Communications 2006*, Bucharest, Romania, June 8–10, 2006, 313–316.

[7] Lellouch, G. and Nikookar, H.
On the capability of a radar network to support communications.
In *Proceedings of SCVT 2007*, Delft, The Netherlands, Nov. 15, 2007.

[8] Fens, R. A. M., Ruggiano, M., and Leus, G.
Channel characterization using radar for transmission of communication signals.
In *Proceedings of the 1st European Wireless Technology Conference*, Amsterdam, The Netherlands, Oct. 27–28, 2008, 127–130.

[9] IEEE Standard Radar Definitions
IEEE Standard 686, 2008.

[10] Poullin, D.
Passive detection using digital broadcasters (DAB, DVB) with COFDM modulation.
IEE Proceedings of Radar Sonar Navigation, **152**, 3 (June 2005), 143–152.

[11] Paichard, Y.
Orthogonal multicarrier phased coded signal for netted radar systems.
In *Proceedings of the 2009 International Waveform Diversity and Design Conference*, Orlando, FL, Feb. 8–13, 2009, 234–236.

[12] Garmatyuk, D., Schuerger, J., Kauffman, K., and Spalding, S.
Wideband OFDM system for radar and communications.
In *Proceedings of the 2009 IEEE Radar Conference*, Pasadena, CA, May 4–8, 2009, 1–6.

[13] Sturm, C., Pancera, E., Zwick, T., and Wiesbeck, W.
A novel approach to OFDM radar processing.
In *Proceedings of the 2009 IEEE Radar Conference*, Pasadena, CA, May 4–8, 2009, 1–4.

[14] Insanic, E. and Siqueira, P.
Velocity unfolding in networked radar system.
In *Proceedings of IGARSS 2008*, vol. 3, Boston, MA, July 7–11, 2008, 1103–1106.

[15] Duan, J., He, Z., and Han, C.
A novel Doppler radar using only two pulses.
In *Proceedings of CIE'06*, Oct. 16–19, 2006, Shanghai, China, 1–4.

[16] Wu, T., Qu, Q., Yuan, S., and Wei, X.
Research on a method of unambiguous velocity measurement of the space surveillance low PRF radars.
In *Proceedings of ISIP 2008*, Moscow, Russia, May 23–25, 2008, 527–532.

[17] Tigrek, R. F., de Heij, W. J. A., and van Genderen, P.
A Method for Measuring the Radial Velocity of a Target with a Doppler Radar.
European Patent Filing No. EP 08162331.6.

[18] Tigrek, R. F., de Heij, W. J. A., and van Genderen, P.
Solving Doppler ambiguity by Doppler sensitive pulse compression using multi-carrier waveform.
In *Proceedings of the 5th European Radar Conference*, Amsterdam, The Netherlands, Oct. 30–31, 2008, 72–75.

[19] Morelli, M., Kuo, C-C. J., and Pun, M-O.
Synchronization techniques for orthogonal frequency division multiple access (OFDMA): a tutorial review.
Proceedings of the IEEE, **95**, 7 (July 2007), 1394–1427.

[20] Franken, G. E. A., Nikookar, H., and van Genderen, P.
Doppler tolerance of OFDM-coded radar signals.
In *Proceedings of the 3rd European Radar Conference*, 2006, 108–111.

[21] Axelsson, S. R. J.
Noise radar using random phase and frequency modulation.
IEEE Transactions on Geoscience Remote Sensing, **42**, 11 (Nov. 2004), 2370–2384.

[22] Levanon, N. and Mozeson, E.
Radar Signals.
Hoboken, NJ: John Wiley, 2004, 42–46.

[23] Wei, W. and Yingning, P.
An interpolation algorithm to improve range estimation for the linear frequency modulated radar.
IEEE Aerospace and Electronics Systems Magazine, **14**, 7 (July 1999), 45–47.

[24] Martin, J.
Range and Doppler accuracy improvement for pulsed Doppler radar.
In *Radar 97*, Edinburgh, UK, Oct. 14–16, 1997, 439–443.

[25] Han, S. H. and Lee, J. H.
An overview of peak-to-average power ratio reduction techniques for multicarrier transmission.
IEEE Wireless Communications, **12**, 2 (Apr. 2005), 56–65.

[26] van den Enden, A. V. M. and Verhoeckx, N. A. M.
Discrete-Time Signal Processing.
New York: Prentice Hall, 1989, 130–138.

[27] Woodward, P. M.
Probability and Information Theory, with Applications to Radar, 2nd ed.
Oxford: Pergamon Press, 1964, 118–120.

R. Firat Tigrek received his B.Sc. and M.Sc. degrees from Middle East Technical University, in Ankara, Turkey, in June 2002 and August 2005, respectively.

From December 2002 to January 2006, he was also with Aselsan Electronic Industries in Ankara, where he worked as an electronic test design engineer. Between March 2006 and March 2009, he joined Thales Nederland as Marie Curie Fellow, and became a Ph.D. candidate at the International Research Center for Telecommunications and Radar (IRCTR) at the Delft University of Technology in Delft, The Netherlands. From March 2009 till January 2010 he continued his Ph.D. as a guest researcher in IRCTR. From January 2010 till February 2011, he was a postdoc researcher at IRCTR, TU Delft. Currently he is a senior radar system engineer at Aselsan Electronic Industries. His research interests involve radar waveform design, radar signal processing, and resource management for radar.

Wim de Heij received his M.Sc. in electrical engineering from Twente University in 1986.

From 1986 to 1990 he worked at Twente University for 4 years as a researcher and achieved his Ph.D. in the field of analog integrated circuit design in 1990. In 1990, he joined Thales Netherlands BV, where he worked in several positions as analog design engineer and system test engineer. Currently he is a principal system design engineer at Thales Netherlands BV.

Piet van Genderen received his M.Sc. degree in electrical engineering from the University of Twente in Enschede, The Netherlands, in 1971. His thesis was in information theory.

After graduation, he joined the National Aerospace Laboratory in Amsterdam, The Netherlands, until 1979. Since then he has been working with Hollandse Signaalapparaten BV in Hengelo, The Netherlands, now Thales Nederland. He held several positions in R&D as group expert radar systems. In 1994 he was appointed full professor at the International Research Centre for Telecommunications and Radar of the Delft University of Technology in the Netherlands. He has (co)authored about 200 papers, seven patents, and a few books. His current research interest is in radar management, adaptable waveforms, and false target recognition.

Professor van Genderen is Member of the European Microwave Association. He has been awarded three times as author/coauthor with the Radar Prize of the European Radar Conference (EuRAD), has received the prize for the most innovative and effective patent of the Thales group, and has received an honorary doctorate of the Military Technical Academy of Romania. He has been the General Chairman of the European Microwave Week in 2004 and the Chairman of the European Microwave Conference during this event. He has been a Member of the Technical Program Committee of numerous international conferences dedicated to radar.